International Journal of Environmental Sciences
ISSN: 2229-7359
Vol. 11 No. 22s, 2025
https://theaspd.com/index.php

Effects of Thermal Radiation and Slip on Heat and Mass Transfer in MHD Nanofluid Flow With Cattaneo-Christov Heat Flux Over a Rotating Disk

A. Bharathi[1], Mattipelli Ramachandru[2], Ch. Kishore Kumar[3], K. Sree Ram reddy[4]
[1]TGSWRDCW, Medak, Telangana, India-502110
[2]UCE&T, Mahatma Gandhi University,Nalgonda, Telangana, India-508254
[3]Department of Mathematics, Nizam College, Osmania University, Telangana, India-500001
[4]Department of Mathematics, UCS, Osmania University, Telangana, India-500007
*corresponding author: bharathi.anam06@gmail.com

Abstract:
This work examines three-dimensional magnetohydrodynamic (MHD) nanofluid flow over a rotating disk, taking into account thermal radiation, thermophoresis, Brownian motion, and the Cattaneo-Christov heat flux model to account for cross-diffusion during heat transmission. Similarity transformations are used to convert the governing equations into nonlinear ODEs, which are then numerically solved using the fourth-order Runge-Kutta method and the bvp4c methodology. The graphical findings indicate how magnetic field, thermal slip, velocity slip, thermophoresis, and Brownian motion affect velocity, temperature, and concentration profiles. Thermal slip reduces velocity, increasing velocity slip results in less uniform temperature distribution, and the combination thermophoresis-Brownian effects have a major impact on thermal and concentration fields.
Key words: *Nanofluid, slip conditions, Cattaneo-Christov heat flux, Thermal radiation.*

1. INTRODUCTION

In the modern era, scientists have made significant progress in improving thermal conductivity and heat transmission. With the rapid advancement of technology, heat transmission has grown in importance in modern times. In order to attain the best outcomes, heat generation is necessary for numerous applications and industries, including manufacturing, transportation, thermal power, and many more. When building different heat transfer components, the low thermal efficiency of the working fluid is a major problem. In order to increase the thermal conductivity of working liquids, several scientists are creating novel techniques. Different components have been proposed by specialists to boost the thermal conductivity of liquids. Therefore, using nonmaterials in working fluids also referred to as nanofluid is a particularly alluring feature. Recent studies on nanofluid have shown some characteristics of a working fluid that contains a combination of nanoparticles. This results from the fact that nanofluids have a higher thermal productivity than working fluids do. The breakthrough liquid known as nanoliquid was first introduced by Choi [1]. A recent assessment of nanliquid's capacity to increase heat transmission rate was provided by Eastman et al. [2]. Electrically conducting fluids and magnetic fields interact in the research of magnetohydrodynamic (MHD) nanofluid flow, which greatly improves heat transfer in a variety of applications. Researchers Farooq et al.[3], Safitri et al. [4], and Nyabuti et al. [5] have examined MHD nanofluids, which are suspensions of nanoparticles in a base fluid, and their distinct thermal and flow properties that are influenced by magnetic fields, temperature-dependent viscosity, and other physical parameters. Abelman et al. [6] reported that increasing the nanoparticle volume fraction improves the thermal conductivity of nanofluids, leading to elevated temperature profiles. Viscous dissipation and Joule heating play a significant role, as they can substantially alter the temperature distribution within the fluid examined in their study. According to study by Khan et al. [7] and Pal et al. [8] changes in thermal conductivity have a significant impact on MHD flows. Nanoparticles like carbon nanotubes and titanium dioxide enhance thermal conductivity and heat transfer rates. MHD and heat radiation interactions have been modeled using sophisticated computational techniques, such as artificial neural networks, which have shown excellent accuracy in forecasting fluid behavior under various circumstances by Akbar et al.[9]. To enhance thermal control, hybrid nanofluids, like those made of Ag-MgO or CuO-MgO, are employed. These fluids have nonlinear thermal radiation and variable viscosity, both of which are essential for maximizing heat transfer processes by Mandal et al. [10] and Vijay & Sharma [11]. In 2023, Mahmud et al. [12] looked at The magnetic field and rotational parameters have a major impact on heat transmission; higher magnetic field intensity increases heat flow at the disk surface. According to study by Sethy et al.

[13] and Khan et al. [14] increasing the disk's angular velocity improves heat transmission because of thermal radiation and convective conditions at the surface.

Heat transport in spinning disk systems is more accurately represented by the Cattaneo-Christov heat flux model, especially in transient situations. Thermal relaxation effects, which are sometimes disregarded in classical Fourier heat conduction, are taken into consideration in this model. When this model is used to research on hybrid nanofluids, it shows notable improvements in flow properties and thermal performance. Non-Fourier heat conduction is incorporated into the model to provide a more accurate representation of heat transfer in fluids with fast temperature fluctuations Shamshuddin et al., [15] According to Ali et al. [16] it is especially helpful in situations involving large magnetic fields and non-Newtonian fluids, when conventional models would not work. Tulu et al., [17] and Mohanty et al.,[18] examines the flow and heat transfer characteristics of a carbon nanotube (CNT)–ethylene glycol nanofluid that is propelled by a flexible, rotating disk. The study takes into account the impact of boundary conditions for thermal and velocity slip, and it looks at how these elements interact when an external magnetic field is applied. The Cattaneo-Christov heat flux formulation is used to more realistically anticipate the temperature distribution and heat conduction within the nanofluid system by precisely modeling the thermal transport mechanism beyond the bounds of Fourier's law.

Taking into consideration the combined impacts of changing viscosity and thermal radiation, Makinde et al. [19] examined the impact of an external magnetic field on the flow behavior of nanoliquids over a convectively heated surface. Their research sheds light on the ways in which these interrelated variables affect fluid dynamics and heat transfer properties in nanoliquid systems. Waqas et al. [20] investigated the impact of heat absorption and generation on the unsteady MHD flow of an Oldroyd-B fluid. To gain a better understanding of how these elements collectively affect the fluid's flow and thermal properties, they included the impacts of thermal radiation into their investigation.

Building on previous research, the current study examines the three-dimensional boundary layer flow of nanofluid over a rotating disk. The impact of heat radiation on flow parameters receives special consideration. The heatflux effect is also included in the thermal conservation equation to account for cross-diffusion processes. The RK-4th order approach is used to obtain numerical solutions, ensuring that computations are accurate and stable. The findings are illustrated with graphical representations of temperature, velocity, and concentration profiles as a function of various controlling parameters. Furthermore, using these graphs, the study investigates and discusses the impacts of magnetic field intensity, thermal slip, thermophoresis, and Brownian motion parameters on flow and heat transfer behavior.

2. Mathematical Formulation

A revolving disk's Maxwell nanoliquid flow has been examined. The analysis will be conducted using the system of cylindrical coordinates (r, ϕ, z). The disk is situated in the z = 0 plane. Moreover, an electrically conducting incompressible nanofluid is present in the half-space $z > 0$. Moreover, slip effects are included. A constant intensity B_0 is applied to the magnetic field in an axial direction. When the induced magnetic field is ignored, the magnetic Reynolds number is extremely low. Whereas T_w is greater than T_∞, T_w stands for wall temperature and T_∞ for ambient temperature. Due of the issue's axial symmetry, the derivatives related to the coordinates ϕ are excluded.

The flow equations used in this investigation are as follows:

$$\frac{\partial u}{\partial r} + \frac{u}{r} + \frac{\partial w}{\partial z} = 0 \tag{1}$$

$$u\frac{\partial u}{\partial r} - \frac{v^2}{r} + w\frac{\partial u}{\partial z} = \left(\frac{\partial^2 u}{\partial r^2} + \frac{1}{r}\frac{\partial u}{\partial r} - \frac{u}{r^2} + \frac{\partial^2 u}{\partial z^2}\right) - \frac{\sigma B_0^2 u}{\rho} \tag{2}$$

$$u\frac{\partial v}{\partial r} - \frac{uv}{r} + w\frac{\partial v}{\partial z} = \left(\frac{\partial^2 v}{\partial r^2} + \frac{1}{r}\frac{\partial v}{\partial r} - \frac{v}{r^2} + \frac{\partial^2 v}{\partial z^2}\right) - \frac{\sigma B_0^2 v}{\rho} \tag{3}$$

$$u\frac{\partial w}{\partial r} + w\frac{\partial w}{\partial z} = \left(\frac{\partial^2 w}{\partial r^2} + \frac{1}{r}\frac{\partial w}{\partial r} + \frac{\partial^2 w}{\partial z^2}\right) \tag{4}$$

$$u\frac{\partial T}{\partial r} + w\frac{\partial T}{\partial z} = \alpha_f\left(\frac{\partial^2 T}{\partial r^2} + \frac{1}{r} + \frac{\partial^2 T}{\partial z^2}\right) + \tau\left(D_B\left[\frac{\partial T}{\partial r}\frac{\partial C}{\partial r} + \frac{\partial T}{\partial z}\frac{\partial C}{\partial z}\right] + \frac{D_T}{T_\infty}\left[\left\{\frac{\partial T}{\partial z}\right\}^2 + \left\{\frac{\partial C}{\partial z}\right\}^2\right]\right) - \frac{\partial q_r}{\partial z} -$$
$$\lambda_1\left(u^2\frac{\partial^2 T}{\partial r^2} + w^2\frac{\partial^2 T}{\partial z^2} + 2uw\frac{\partial^2 T}{\partial r\,\partial z} + \frac{\partial T}{\partial r}\left(u\frac{\partial u}{\partial r} + w\frac{\partial u}{\partial z}\right) + \frac{\partial T}{\partial z}\left(u\frac{\partial w}{\partial r} + w\frac{\partial w}{\partial z}\right)\right) \tag{5}$$

$$u\frac{\partial C}{\partial r} + w\frac{\partial C}{\partial z} = D_B\left(\frac{\partial^2 C}{\partial r^2} + \frac{1}{r}\frac{\partial C}{\partial r} + \frac{\partial^2 C}{\partial z^2}\right) + \left(\frac{D_T}{T_\infty}\right)\left(\frac{\partial^2 T}{\partial r^2} + \frac{1}{r}\left(\frac{\partial T}{\partial r}\right) + \frac{\partial^2 T}{\partial z^2}\right) \tag{6}$$

The present investigation's boundary settings are as follows:

$$u = L_1\frac{\partial u}{\partial z}, v = r\Omega + L_1\frac{\partial v}{\partial z}, w = o, T = T_W + L_2\frac{\partial T}{\partial z}, C = C_w + L_3\frac{\partial C}{\partial z}\ \text{at}\ z = 0$$
$$u \to 0, v \to 0, T \to \infty, C \to \infty\ \text{as}\ z \to \infty \quad (7)$$

The Radiative heat flux q_r is equal to when radiation is evaluated using the Rosseland approximation.

$$q_r = -\frac{2\sigma^*}{3k^*}\frac{\partial T}{\partial z} = -\frac{16\sigma^* T_\infty^3}{3k^*}\frac{\partial^2 T}{\partial z^2} \quad (8)$$

The mean absorption coefficient is denoted by k^*, and the Stefan-Boltzmann constant is represented by σ^*. In a Taylor series, extending T^4 about T_∞ while disregarding higher order terms, we have

$$T^4 \cong 4T_\infty^3 T - 3T_\infty^4 \quad (9)$$

We take into account the following transformations of similarity.

$$u = r\Omega F'^{(\eta)}, v = r\Omega G(\eta), w = -\sqrt{2\nu_f\Omega}F(\eta), \eta = \sqrt{\frac{2\Omega}{\nu_f}}z$$
$$T = T_\infty + [T_w - T_\infty]\Theta(\eta), C = C_\infty + [C_w - C_\infty]\Phi(\eta) \quad (10)$$

Equations (2), (3), (5), and (6) take on a new form when Eq. (10) is used.

$$F''' - MF' + FF'' + \frac{1}{2}G^2 - \frac{1}{2}F'^2 = 0 \quad (11)$$

$$G'' + FG' - F'G - MG = 0 \quad (12)$$

$$\left(1 + \frac{4N}{3} + \gamma PrF^2\right)\Theta'' + Pr(Nb\Theta'\Phi' + Nt\Theta'^2 - F\Theta' + \gamma FF'\Theta') = 0 \quad (13)$$

$$\Phi'' + \frac{Nt}{Nb}\Theta'' + ScF\Phi' = 0 \quad (14)$$

Boundary conditions becomes as:

$$F(0) = 0, \alpha_1 F''(0) = F'(0), 1 + \alpha_1 G'(0) = G(0), 1 + \alpha_2\Theta'(0) = \Theta(0), 1 + \alpha_3\Phi'(0) = \Phi(0) \text{at}\ \eta = 0 \text{ and } F \to 0, G \to 0, \Theta \to 0, \Phi \to 0 \text{ as } \eta \to \infty \quad (15)$$

Here, Tangential stress $\tau_\theta = \mu\left(\frac{\partial v}{\partial z}\right)_{z=0} = \mu r\Omega\sqrt{\frac{2\Omega}{\nu_f}}G'(0)$,

Radial stress $\tau_r = \mu\left(\frac{\partial u}{\partial r} + \frac{\partial w}{\partial r}\right)_{z=0} = \mu r\Omega\sqrt{\frac{2\Omega}{\nu_f}}F''(0)$,

Skin friction coefficienr $C_f = \frac{\sqrt{\tau_r^2 + \tau_\theta^2}}{\rho(r\Omega)^2} = \sqrt{\frac{2\nu}{r^2\Omega}}\sqrt{F''^2(0) + G''^2(0)}$ (16)

Local Nusselt number $Nu_x = \frac{\left(\frac{\partial T}{\partial z}\right)_{z=0}}{(T_W - T_\infty)} = -\sqrt{\frac{2\Omega}{\nu_f}}\Theta'(0)$ (17)

3. RESULTS AND DISCUSSIONS

When applied to the boundary conditions (15), the coupled nonlinear ordinary differential equations (11–14) are numerically solved using the RK-4th order method (bvp4c numerical Method). The following are numerical results for pertinent physical parameters: M is for magnetic field, Pr is for Prandtl number, Sc is for Schmidt number, Nb is for Brownian motion parameter, N is for radiation, gamma is for thermal relaxation time factor, and Nt is for Thermophoresis parameter.

Table.1 was constructed and a descending contrast was recovered in order to verify the validity of the current results with published studies. Additionally, Table 2 shows variations in the energy transfer rate versus various flow model including elements. Thermophoretic effects increase the energy transfer ratio because the deep penetration of nanoparticles in the liquid thickens the thermal boundary layer. The local Nusselt number falls as the thermal slip coefficient rises. In comparison, the Prandtl number contrasts the momentum and heat diffusion coefficients. Through thermal diffusivity, thermal boundary layer thickness is influenced. Comparing fluids with a higher Prandtl number (Pr) to those with a lower Pr, the former exhibit a stronger thermal boundary effect and only a minor increase in boundary layer thickness due to the lower thermal diffusivity. A steeper temperature gradient close to the wall is the result of a thicker thermal barrier layer.

Table.1: $F'(0), \& G(0)$ for various values slip and M

M	α_1	Mustafa [23]		Present	
		$F''(0)$	$-G(0)$	$F''(0)$	$-G(0)$
0	0.25	0.259534	0.146784	0.25876	0.14665
0.2	0.25	0.191176	0.509536	0.19367	0.51068

0.4	0.25	0.146057	0.599523	0.14899	0.61342
0.6	0.25	0.116699	0.680355	0.12883	0.68035
0.5	0	0.218678	0.755935	0.21623	0.75593
0.5	0.2	0.143038	0.662149	0.14238	0.66215
0.5	0.4	0.099146	0.584589	0.10536	0.58451
0.5	0.6	0.071917	0.522031	0.07682	0.52209

Table.2: valus of modified Nusselt number for various values Nt, Nb, Pr, N, γ

Pr	Nt	Nb	γ	N	$-\Theta'(0)$
4	0.2	0.1	0.1	0.2	0.4502
5					0.3614
6					0.2993
7	0.3				0.19605
7	0.4				0.1635
7		0.2			0.4863
7		0.3			0.3657
7			0.3		0.4752
7			0.4		0.4853
7			0.5	0.3	0.4992
7				0.5	0.4063

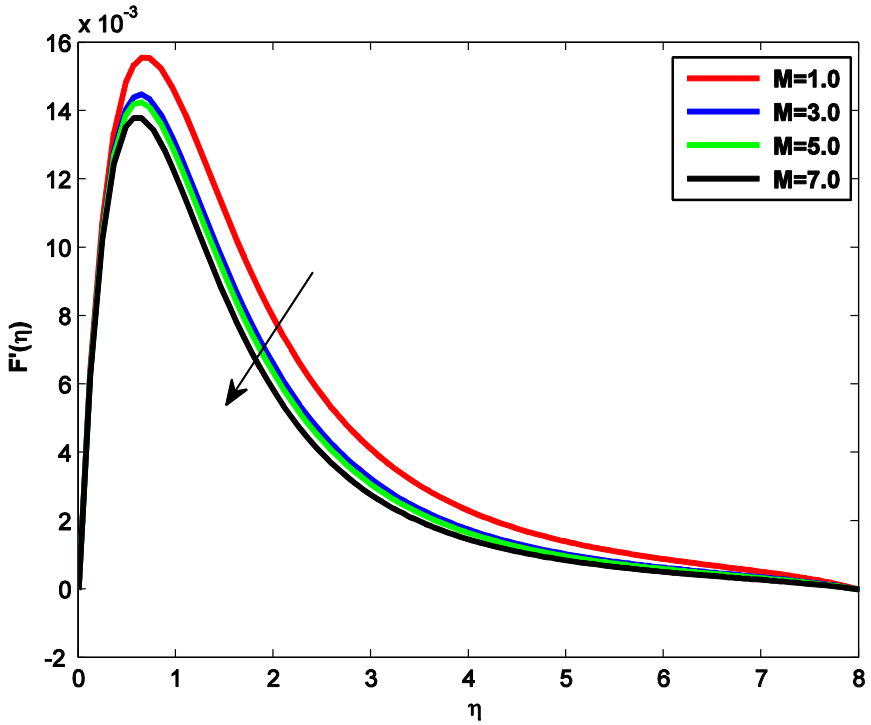

Fig. 1 Magnetic parameter verses Radial Velocity

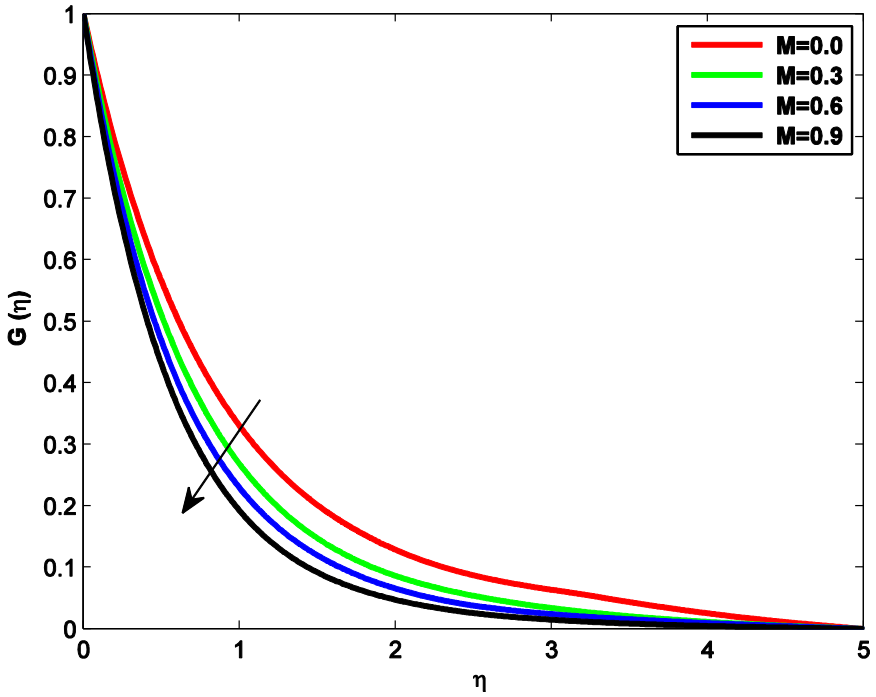

Fig.2 Magnetic parameter verses Azimuthal Velocity

The fluctuation of the azimuthal and radial velocity profiles with respect to the magnetic field parameter M is shown in Figure 1&2. A decrease in fluid mobility in the radial direction is indicated by the suppression of the radial velocity caused by the Lorentz force generated by the magnetic field. On the other hand, the azimuthal velocity decreases with increasing magnetic field strength and shows an inverse relationship on M.

Figure 3 shows how the radial profiles change with the velocity slip parameter α_1 for a specific magnetic parameter M. The primary cause of the disk's non-null radial velocity due to slip is centrifugal forces. The external flux keeps moving radially outward, but the radial velocity decreases as α_1 increases, reaching its maximum as it moves toward the disk's surface.

Figure 4 displays in a nanofluid, the thermophoresis parameter Nt describes the ratio of momentum dispersion to diffusion of nanoparticles through the thermophoretic force. When exposed to a temperature gradient, nanoparticles frequently move from one hot area to another cold area. An increase of Nt in the thermophoresis parameter results in wider profiles, which indicates an expanded thermal boundary layer. The thermal slip parameter affects the thermal boundary layer is shown in Fig. 5. A higher value results in a lower temperature because less heat is transported from the disc to the adjacent zones of the fluids. The profile of temperature Fig.6 demonstrates that a greater value of Nb is associated with a higher temperature profile $\Theta(\eta)$.

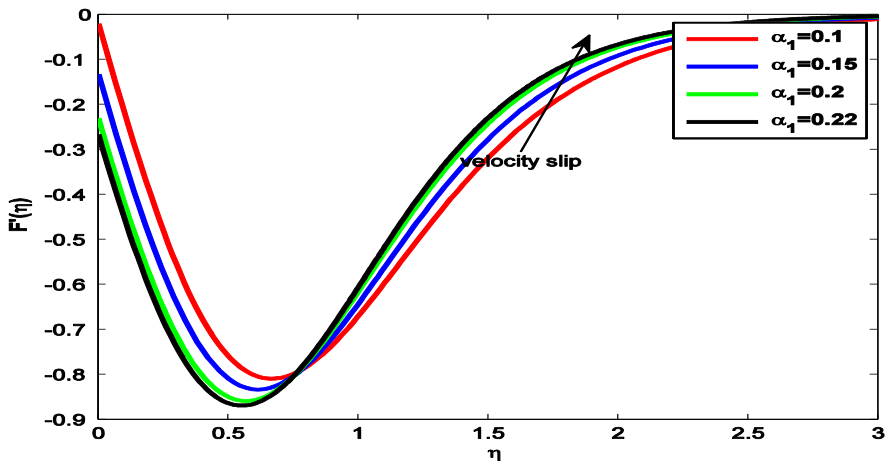

Fig.3 Radial velocity verses Velocity slip

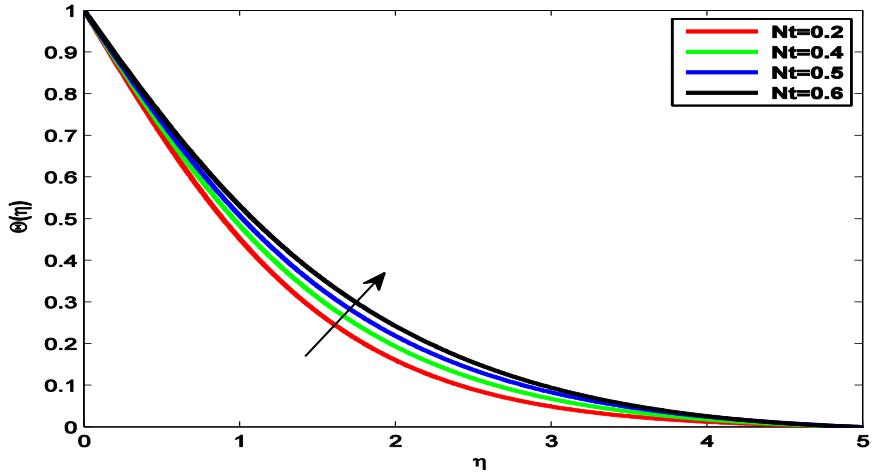

Fig.4 Temperature verses Nt

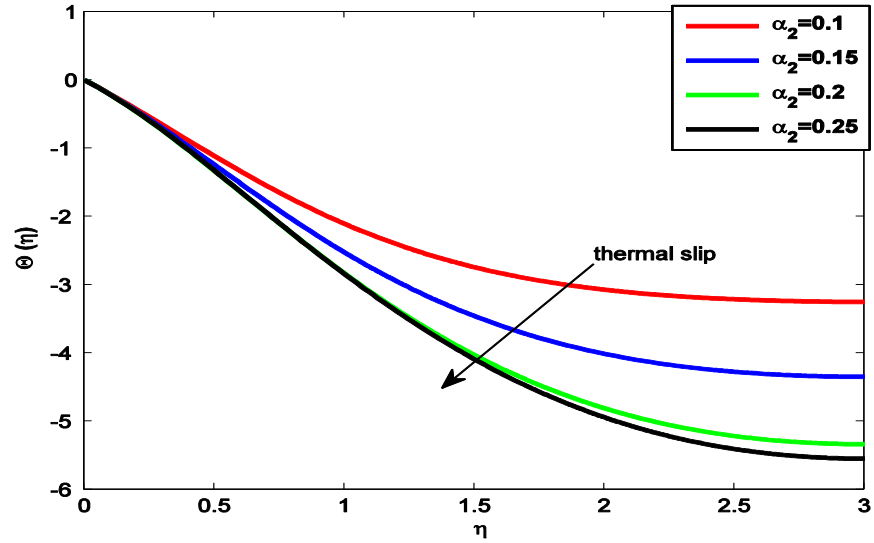

Fig. 5 Temperature profile verses Thermal slip

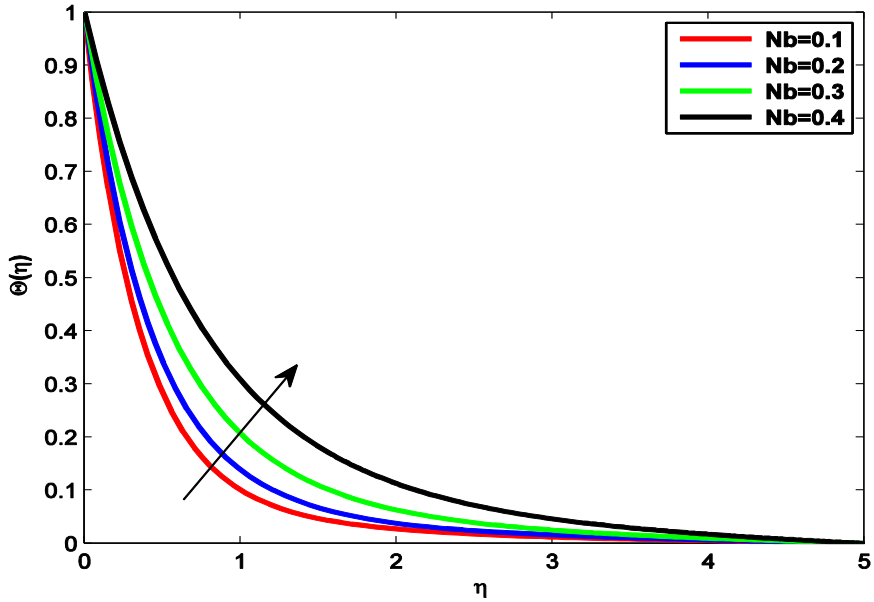

Fig. 6 Temperature verses Nb

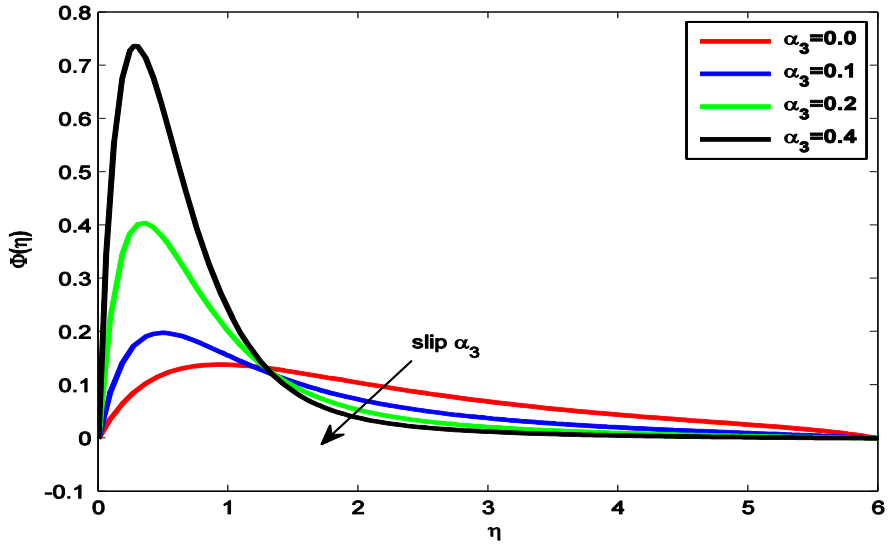

Fig.7 concentration verses slip parameter

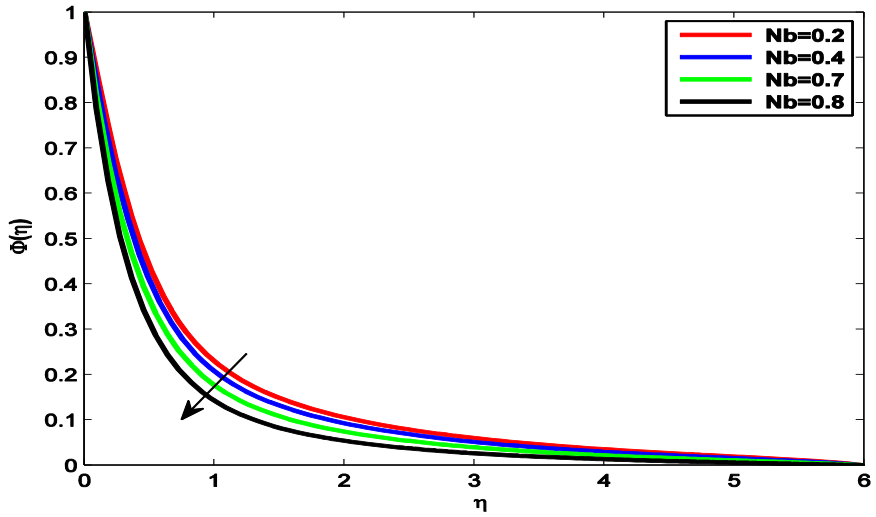

Fig. 8 Concentration profile verses Nb

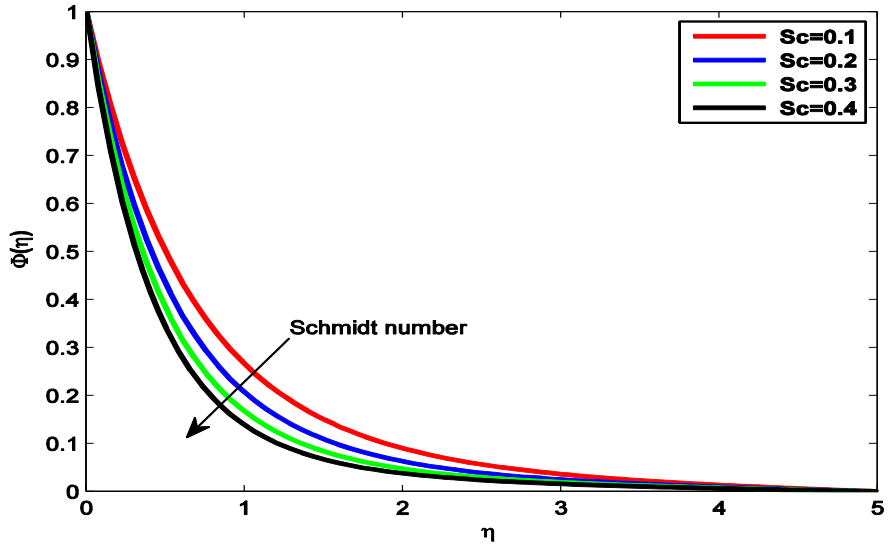

Fig. 9 Concentration profile verses Sc

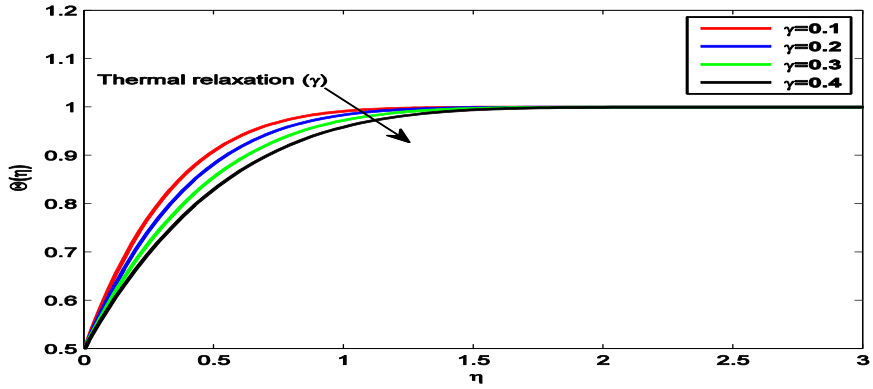

Fig.10 Temperature verses thermal relaxation

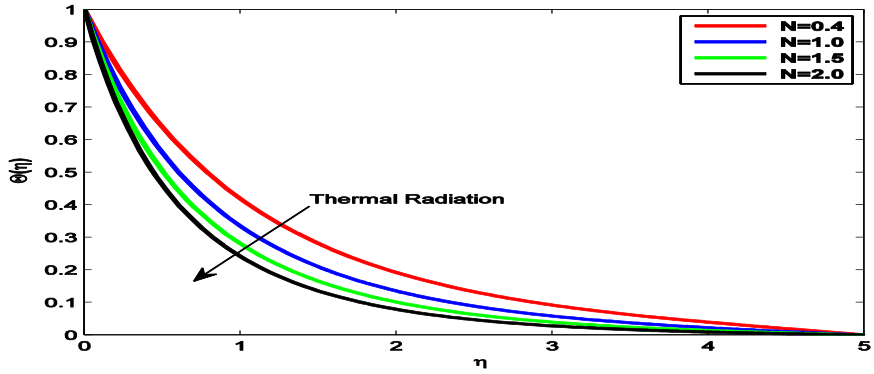

Fig.11 temperature verses thermal radiation (N)

The thermal slip parameter (α) is plotted against the concentrations given by Φ(η) in Figure 7 The function Φ significantly reduces as the parameter a broadens, and the profiles finest point also shifts in the direction of the wall. Furthermore, as the Brownian motion parameter Nb increased, the resulting concentration profile significantly decreased, as shown in Fig. 8.

Fig. 9 illustrates how greater Schmidt numbers Sc result in shorter concentration boundary layers and a larger concentration gradient Φ'(0) on the surface because of their inverse relationship with the Brownian diffusion coefficient D_B.

The temperature profiles in Fig.10 show that improved insulating efficacy is achieved with higher thermal relaxation values, which emphasize the medium particles requirement for more time to transfer heat to their surrounding particles. Cause the fluid's temperature to noticeably drop.

While renewing nanoparticles, N modifies the temperature on a revolving disk, as seen in Fig. 11 Actually, radiation is incorporated into temperature. The champ amplifies the Brownian development. Additionally, the constant presence of small nanoparticles will frequently cause the fluid's temperature to rise.

4. CONCLUSIONS

i. As the velocity slip factor rises, the momentum boundary layer's thickness falls.

ii. A greater thermal slip factor tends to counteract heat transfer from the fluid towards the disk surface and reduce the temperature distribution at the disk wall.

iii. The thermal boundary becomes weaker after a temperature increase because more heat can diffuse through the fluid.

REFERENCES:

1. Choi, S. U. S. (2009). Nanofluids: From vision to reality through research. Journal of Heat Transfer, 131(3). https://doi.org/10.1115/1.3056479

2. Eastman, J., Phillpot, S., Choi, S., & Keblinski, P. (2004). THERMAL TRANSPORT IN NANOFLUIDS. Annual Review of Materials Research, 34(1), 219–246. https://doi.org/10.1146/annurev.matsci.34.052803.090621

3. Farooq, U., Akhtar, K., Abbasi, M. M., Hussain, M., & Aldandani, M. (2023). Convective heat transfer performance of MHD nanofluid flow with temperature dependent viscosity over stretching surface. ZAMM - Journal of Applied Mathematics and Mechanics / Zeitschrift Für Angewandte Mathematik Und Mechanik, 103(10). https://doi.org/10.1002/zamm.202300053

4. Safitri, O., Widodo, B., Adzkiya, D., & Kamiran, K. (2020). Unsteady magnetohydrodynamics mixed convection flow pass sliced magnetic sphere in nano fluid. AIP Conference Proceedings, 2242, 030021. https://doi.org/10.1063/5.0007933

5. Nyabuti, V., Kiogora, P. R., Onyango, E., & Nyawade, E. (2024). Unsteady MHD Nanofluid Flow through a Divergent Conduit with Chemical Reaction and Radiation. International Journal of Fluid Mechanics & Thermal Sciences, 10, 1-14.
6. Abelman, S., Sayehvand, H. O., & Parsa, A. (2017). Mhd nanofluid flow with viscous dissipation and joule heating through a permeable channel. Frontiers in Heat and Mass Transfer (FHMT), 9(1).
7. Khan, Z., Srivastava, H. M., Mohammed, P. O., Jawad, M., Jan, R., & Nonlaopon, K. (2022). Thermal boundary layer analysis of MHD nanofluids across a thin needle using non-linear thermal radiation. Mathematical Biosciences & Engineering, 19(12), 14116–14141. https://doi.org/10.3934/mbe.2022658
8. Pal, D., Mandal, G., Vajravelu, K., & Al-Kouz, W. (2023). MHD thermo-radiative heat transfer characteristics of carbon nanotubes based nanofluid over a convective expanding sheet in a porous medium with variable thermal conductivity. International journal of modeling and Simulation,1-12. https://doi.org/10.1080/02286203.2023.2237847
9. Akbar, A., Ullah, H., Raja, M. a. Z., Nisar, K. S., Islam, S., & Shoaib, M. (2022). A design of neural networks to study MHD and heat transfer in two phase model of nano-fluid flow in the presence of thermal radiation. Waves in Random and Complex Media, 1–24. https://doi.org/10.1080/17455030.2022.2152905
10. Mandal, S., Mukherjee, S., Shit, G. C., & Vajravelu, K. (2024). Entropy analysis of MHD flow in hybrid nanofluid over a rotating disk with variable viscosity and nonlinear thermal radiation. ZAMM - Journal of Applied Mathematics and Mechanics / Zeitschrift Für Angewandte Mathematik Und Mechanik. https://doi.org/10.1002/zamm.202301027
11. Vijay, N., & Sharma, K. (2022). Magnetohydrodynamic hybrid nanofluid flow over a decelerating rotating disk with Soret and Dufour effects. Multidiscipline Modeling in Materials and Structures, 19(2), 253–276. https://doi.org/10.1108/mmms-08-2022-0160
12. Mahmud, K., Duraihem, F. Z., Mehmood, R., Sarkar, S., & Saleem, S. (2023). Heat transport in inclined flow towards a rotating disk under MHD. Scientific Reports, 13(1). https://doi.org/10.1038/s41598-023-32828-6
13. Sethy, P., Kumar, A., Ray, A. K., Kumari, A., & Tlau, L. (2024). Synergistic impacts of radiative flow of Maxwell fluid past a rotating disk with reactive conditions: An Arrhenius model analysis. Chinese Journal of Physics, 89, 761–792. https://doi.org/10.1016/j.cjph.2024.03.018
14. Khan, M., Ahmed, J., & Ali, W. (2020). Thermal analysis for radiative flow of magnetized Maxwell fluid over a vertically moving rotating disk. Journal of Thermal Analysis and Calorimetry, 143(6), 4081–4094. https://doi.org/10.1007/s10973-020-09322-6
15. Shamshuddin, M., Salawu, S., Bég, O. A., Usman, N., Bég, T. A., & Kuharat, S. (2024). Numerical study of electroconductive non-Newtonian hybrid nanofluid flow from a stretching rotating disk with a Cattaneo–Christov heat flux model. Proceedings of the Institution of Mechanical Engineers Part E Journal of Process Mechanical Engineering. https://doi.org/10.1177/09544089241258019
16. Ali, U., Irfan, M., Rehman, K. U., Alqahtani, A. S., Malik, M. Y., & Shatanawi, W. (2022). On the Cattaneo–Christov heat flux theory for mixed convection flow due to the rotating disk with slip effects. Waves in Random and Complex Media, 1–15. https://doi.org/10.1080/17455030.2022.2056659
17. Tulu, A., & Ibrahim, W. (2020). MHD Slip Flow of CNT-Ethylene Glycol Nanofluid due to a Stretchable Rotating Disk with Cattaneo–Christov Heat Flux Model. Mathematical Problems in Engineering, 2020, 1–13. https://doi.org/10.1155/2020/1374658
18. Mohanty, D., Mahanta, G., & Shaw, S. (2023). Analysis of irreversibility for 3-D MHD convective Darcy–Forchheimer Casson hybrid nanofluid flow due to a rotating disk with Cattaneo–Christov heat flux, Joule heating, and nonlinear thermal radiation. Numerical Heat Transfer Part B-Fundamentals, 84(2), 115–142. https://doi.org/10.1080/10407790.2023.2189644
19. Makinde, O. D., Mahanthesh, B., Gireesha, B. J., Shashikumar, N., Monaledi, R., & Tshehla. (2018). MHD Nanofluid Flow Past a Rotating Disk with Thermal Radiation in the Presence of Aluminum and Titanium Alloy Nanoparticles. Defect and Diffusion Forum/Diffusion and Defect Data, Solid State Data. Part a, Defect and Diffusion Forum, 384, 69–79. https://doi.org/10.4028/www.scientific.net/ddf.384.69
20. Waqas, H., Imran, M., Muhammad, T., Sait, S. M., & Ellahi, R. (2020). Numerical investigation on bioconvection flow of Oldroyd-B nanofluid with nonlinear thermal radiation and motile microorganisms over rotating disk. Journal of Thermal Analysis and Calorimetry, 145(2), 523–539. https://doi.org/10.1007/s10973-020-09728-2
21. Mustafa, M. (2017a). MHD nanofluid flow over a rotating disk with partial slip effects: Buongiorno model. International Journal of Heat and Mass Transfer, 108, 1910–1916. https://doi.org/10.1016/j.ijheatmasstransfer.2017.01.064